Computation of Spray Dynamics by Direct Solution of Moment Transport Equations–Inclusion of Nonlinear Momentum Exchange

M. R. Archambault[*]
Propulsion Sciences and Advanced Concepts Division
Air Force Research Laboratory
Edwards AFB, CA 93524 USA

C. F. Edwards
Department of Mechanical Engineering
Stanford University
Stanford, CA 94305 USA

Abstract

Using conventional particle tracking techniques to predict the dynamics of spray flows can be prohibitively expensive, requiring large computation times and significant data storage. Moreover, because of the discontinuous nature of the spray drops, data from a simulation of the flow does not produce smooth statistics unless the results from many simulations have been averaged. Recently, a new model was developed that computes spray statistics directly, without simulating the flow. In this paper, the model is extended to include the effects of nonlinear momentum exchange between the phases. The approach was tested on a quasi-one-dimensional flow geometry. The results are compared with a Lagrangian simulation and demonstrate good agreement.

Introduction

Spray flows play an important role in many industrial processes today. It is therefore vital that we have a full understanding of the physics of these flows and are able to accurately predict both the distribution and behavior of the drops and the dynamics of the gas phase. Failure to adequately model these flows could lead to inefficient fuel mixing, non-uniform industrial coatings, or poorly distributed agricultural sprays. Additionally, since one may wish to make small changes to an engine or injector design to determine the effects on the two-phase mixture, it is of significant interest to reduce the time required to predict these spray flows.

Perhaps the most common approach to studying spray flows has been the Lagrangian-Eulerian, or particle-tracking method.[1,2,3,4] Drops are stochastically injected into the gas phase and their trajectories are determined by integrating a Lagrangian equation of motion. The gas phase is typically modeled with the time-dependent RANS equations with a suitable turbulence model and exchange terms.

While particle-tracking methods have provided useful information in many applications, they have some potentially significant drawbacks. For instance, data arising from a simulation must be post-processed. If the quantity of interest is the mean number density in each grid cell, this may not pose a problem. However, if we are interested in more detailed statistics, the required computational time increases because a sufficient number of drops must pass through the cell to provide a data set large enough for a meaningful average. As the quantity of interest becomes more specific, the necessary computation time becomes more prohibitive.

An alternative approach which does not involve simulation is to compute the evolution of a probability density function (PDF) describing the drops. Williams[5] was the first to derive a transport equation for a droplet PDF, called the spray equation, analogous to Boltzmann's equation for molecules. Direct solutions of the spray equation have been attempted,[6,7,8,9,10] but only with limited success. The high-dimensionality of the equation and current computational resources limit the numerical resolution attainable within the phase space.

Recently, a Maximum Entropy Moment Closure (MEMC) model was described that gives a complete description of a spray flow by computing the evolution of its PDF along with the gas flow in which it is embedded.[11] It was shown that both general and detailed statistics about the spray drops and the solution of the gas phase could be attained without the need to average simulation data and in significantly less time than might be required in a typical particle-tracking method. The purpose of this paper is to incorporate a nonlinear drag law into the model and compare test results to a Lagrangian simulation.

---

[*] Corresponding author

20000830 079

DTIC QUALITY INSPECTED 4

Governing Equations

The equations that describe the evolution of our system make use of ensemble averaging which is independent of any time or length scales. They also restrict us to single-point statistics.[12] Each drop is described by a relatively small set of characteristics which contains the information of interest. This set of characteristics describes a state vector $\bar{\alpha}$ whose elements define the axes of a hyperspace, called $\bar{\alpha}$-space, through which the drop can move.

Because we are dealing with point particles, volume displacement effects are negligible, and we are able to treat any interphase exchange as if the drop were alone in a locally uniform gas field.

With these assumptions, a probabilistic description of the spray can be developed,[12] defining $\lambda(\bar{x};t)^{\dagger}$ as the probability density of finding a single drop in the vicinity of a point $(\bar{x},t)$. It is also the expected number density of drops at $\bar{x}$ and t. This dual interpretation is important since we are generally more interested in the expected number density rather than the probability density. The probabilistic description also defines the function $f(\bar{\alpha}';\bar{x},t)$, the probability density of finding a particular diameter and velocity. This is conditioned on a drop existing at $\bar{x}$ and t, and $\bar{\alpha}'$-space is the subset of $\bar{\alpha}$-space excluding the spatial coordinate. By combining these two functions, we define the unnormalized single-particle probability density function for the spray

$$F(\bar{\alpha};t)d\bar{\alpha} = \lambda(\bar{x};t)f(\bar{\alpha}';\bar{x},t)d\bar{\alpha}'dV \qquad (1)$$

$F(\bar{\alpha};t)$ is unnormalized because $\lambda(\bar{x};t)$, also an unnormalized PDF, determines how much spray is present at $\bar{x}$ and t.

If $\bar{\alpha} = (\bar{x},\phi,\bar{v},T)$, a transport equation for $F(\bar{\alpha};t)$ can now be derived.[13,14,15]

$$\frac{\partial F}{\partial t}+\nabla_x \cdot (F\bar{v})+\nabla_v \cdot (F\bar{a})$$
$$+\frac{\partial}{\partial \phi}(F\Phi)+\frac{\partial}{\partial T}(F\Theta) = \dot{S}_2 + \dot{S}_1 + \dot{S}_0 \qquad (2)$$

Equation (2) is the spray equation. It describes the evolution of the probability density function $F(\bar{x},\phi,\bar{v},T;t)$ through joint physical, diameter,

† For clarity when denoting a PDF, those arguments over which the function is a density will be listed first, followed by a semi-colon, followed by arguments that are parameters of the function.

velocity, and temperature space and includes source terms accounting for binary collision S_2, unary breakup S_1, and zero-body events S_0 such as nucleation and complete vaporization. The spray equation has not generally been viewed as a practical way of predicting spray flows. It is an unusual evolution equation in the sense that the quantity of interest is not only being transported through physical space, but also through diameter, velocity, and temperature space. A numerical solution requires a full discretization of this hyperspace, making a direct solution difficult.

Considering a non-vaporizing, isothermal spray without collisions, breakup, or zero-body events, the spray equation reduces to

$$\frac{\partial F}{\partial t}+\nabla_x \cdot (F\bar{v})+\nabla_v \cdot (F\bar{a})=0 \qquad (3)$$

The diameter axis is then discretized into equal-sized bins, taking the approach of Tambour.[16] By splitting and integrating equation (3),[11] a set of velocity moment transport equations within each diameter bin can be derived as

$$\frac{\partial (\lambda_n \langle v_x \rangle_n)}{\partial t}+\nabla_x \cdot (\lambda_n \langle \bar{v}v_x \rangle_n) = \frac{\lambda_n}{\Delta\phi_n}\langle a_x \rangle_n \qquad (4)$$

$$\frac{\partial (\lambda_n \langle v_x^2 \rangle_n)}{\partial t}+\nabla_x \cdot (\lambda_n \langle \bar{v}v_x^2 \rangle_n) = 2\frac{\lambda_n}{\Delta\phi_n}\langle a_x v_x \rangle_n \qquad (5)$$

$$\frac{\partial (\lambda_n \langle v_y \rangle_n)}{\partial t}+\nabla_x \cdot (\lambda_n \langle \bar{v}v_y \rangle_n) = \frac{\lambda_n}{\Delta\phi_n}\langle a_y \rangle_n \qquad (6)$$

$$\frac{\partial (\lambda_n \langle v_y^2 \rangle_n)}{\partial t}+\nabla_x \cdot (\lambda_n \langle \bar{v}v_y^2 \rangle_n) = 2\frac{\lambda_n}{\Delta\phi_n}\langle a_y v_y \rangle_n \qquad (7)$$

$$\frac{\partial (\lambda_n \langle v_x v_y \rangle_n)}{\partial t}+\nabla_x \cdot (\lambda_n \langle \bar{v}v_x v_y \rangle_n)$$
$$=\frac{\lambda_n}{\Delta\phi_n}(\langle a_x v_y \rangle_n + \langle a_y v_x \rangle_n) \qquad (8)$$

To determine the droplet diameter distribution, an evolution equation for the binned droplet number density is solved

$$\frac{\partial \lambda_n}{\partial t} + \nabla_x \cdot \left(\lambda_n \langle \mathbf{v}_x \rangle_n \right) = 0 \qquad (9)$$

λ_n is the probability of finding a drop in the vicinity of some spatial point at some instant in time within the nth diameter bin. The overall droplet number density is given by

$$\lambda = \sum_n \lambda_n \qquad (10)$$

The terms on the right sides of equations (4) through (8) account for the momentum exchange between the gas and liquid phases. The acceleration term $\bar{a}$ is given by

$$\bar{a} = \frac{-\frac{1}{2} C_D \rho_g |\bar{\mathbf{v}} - \bar{u}| (\bar{\mathbf{v}} - \bar{u}) \pi \frac{\phi^2}{4}}{\rho_l \frac{\pi}{6} \phi^3} \qquad (11)$$

where

$$C_D = \frac{24}{\mathrm{Re}} \left(1 + 0.15 \mathrm{Re}^{0.687} \right) \qquad (12)$$

giving

$$\bar{a} = -\frac{18 \rho_g v_g}{\rho_l \phi^2} \left[1 + 0.15 \left(\frac{|\bar{\mathbf{v}} - \bar{u}| \phi}{v_g} \right)^{0.687} \right] (\bar{\mathbf{v}} - \bar{u}) \qquad (13)$$

Defining $\bar{g} = \bar{\mathbf{v}} - \bar{u}$ as the slip velocity, the x-component of the expected acceleration in the nth diameter bin is

$$\langle a_x \rangle_n = -\frac{1}{\tau_n} \left(\langle \mathbf{v}_x \rangle_n - \langle u_x \rangle \right) \Delta \phi_n$$
$$- \frac{2.7 \rho_g v^{0.313}}{\Delta \phi_n \rho_l} \left(\phi_1^{-0.313} - \phi_2^{-0.313} \right) \left\langle |\bar{g}|^{0.687} g_x \right\rangle_n \qquad (14)$$

where

$$\tau_n = \frac{\rho_l \phi_{geo,n}^2}{18 \rho_g v_g} \qquad (15)$$

is the representative droplet relaxation time of the nth diameter bin and ϕ_1 and ϕ_2 are the starting and ending diameters of the bin, and $\phi_{geo,n} = \sqrt{\phi_1 \phi_2}$. Similarly,

$$\langle a_x \mathbf{v}_x \rangle_n = -\frac{1}{\tau_n} \left(\langle \mathbf{v}_x^2 \rangle_n - \langle u_x \mathbf{v}_x \rangle_n \right) \Delta \phi_n$$
$$- \frac{5.4 \rho_g v^{0.313}}{\Delta \phi_n \rho_l} \left(\phi_1^{-0.313} - \phi_2^{-0.313} \right) \left\langle |\bar{g}|^{0.687} g_x \mathbf{v}_x \right\rangle_n \qquad (16)$$

Quasi-One-Dimensional Spray Problem

Because we are interested in a spray problem that is understandable, physically interesting, and tractable while at the same time being able to evaluate the spray model, we make use of a quasi-one-dimensional flow. Figure 1 shows the geometry for this problem. At $x = 0$ there is a two-dimensional array of spray
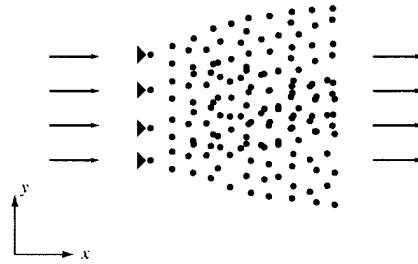

Figure 1 Geometry for quasi-1D spray flow

injectors that extends infinitely in the y-direction. Each injector delivers a distribution of drops into an incompressible gas, which initially has a low level of turbulence. The array and each injector on it extend infinitely in the z-direction, resulting in a series of wedge sprays of spherical drops.

Now imagine an ensemble of these arrays.[‡] Because we wish to develop a quasi-one-dimensional flow, we restrict the PDF for the drop velocities at each injector to have a mean transverse (y-direction) velocity of zero. If there is an infinite number of realizations in the ensemble, then there is no preferential location along the transverse axis since there is equal probability for a drop to have a positive y-velocity of some magnitude as there is for a drop to have a negative y-velocity of the same magnitude. Similarly, we have a zero-mean gas velocity component in the y-direction, though fluctuations do occur. Because there is no preferential location along the transverse axis, there are no variations along that axis across the ensemble, and therefore, derivatives of averaged quantities in the y-

[‡] To ensure a quasi-one-dimensional geometry, two approaches can be taken with the injectors. First, in each realization of the ensemble, the injectors can be placed on the array at random. Alternatively, the injectors could be equally spaced on each array, but shifted slightly from one realization to another. In either case, the flow will be quasi-one-dimensional across the ensemble.

direction are zero. So, the three primary constraints for this problem are

$$\langle u_y \rangle = 0, \quad \langle v_y \rangle = 0, \quad \frac{\partial \langle \ \rangle}{\partial y} = 0 \qquad (17)$$

Also, so that no mean flow develops in the transverse direction, there can be no correlation between the x- and y-components of velocity in either phase. Thus, all cross-component and cross-component/cross-phase moments are zero. Substituting these constraints into the transport equations yields

$$\frac{\partial \lambda_n}{\partial t} + \nabla_x \cdot \left(\lambda_n \langle v_x \rangle_n \right) = 0 \qquad (18)$$

$$\frac{\partial \left(\lambda_n \langle v_x \rangle_n \right)}{\partial t} + \frac{\partial \left(\lambda_n \langle v_x^2 \rangle_n \right)}{\partial x}$$
$$= -\frac{\lambda_n}{\tau_n} \left(\langle v_x \rangle_n - \langle u_x \rangle \right) \qquad (19)$$
$$- \frac{8.6 \lambda_n}{\Delta \phi_n} \rho_g \nu_g^{0.313} \left(\phi_1^{-0.313} - \phi_2^{-0.313} \right) \left\langle \left| \vec{g} \right|^{0.687} g_x \right\rangle_n$$

$$\frac{\partial \left(\lambda_n \langle v_x^2 \rangle_n \right)}{\partial t} + \frac{\partial \left(\lambda_n \langle v_x^3 \rangle_n \right)}{\partial x}$$
$$= -\frac{\lambda_n}{\tau_n} \left(\langle v_x^2 \rangle_n - \langle u_x v_x \rangle_n \right) \qquad (20)$$
$$- \frac{17.2 \lambda_n}{\Delta \phi_n} \rho_g \nu_g^{0.313} \left(\phi_1^{-0.313} - \phi_2^{-0.313} \right) \left\langle \left| \vec{g} \right|^{0.687} g_x v_x \right\rangle_n$$

$$\frac{\partial \left(\lambda_n \langle v_y^2 \rangle_n \right)}{\partial t} + \frac{\partial \left(\lambda_n \langle v_x v_y^2 \rangle_n \right)}{\partial x}$$
$$= -\frac{\lambda_n}{\tau_n} \left(\langle v_y^2 \rangle_n - \langle u_y v_y \rangle_n \right) \qquad (21)$$
$$- \frac{17.2 \lambda_n}{\Delta \phi_n} \rho_g \nu_g^{0.313} \left(\phi_1^{-0.313} - \phi_2^{-0.313} \right) \left\langle \left| \vec{g} \right|^{0.687} g_y v_y \right\rangle_n$$

If constraints (17) are applied to the incompressible RANS equations, we obtain

$$\frac{\partial \langle u_x \rangle}{\partial x} = 0 \qquad (22)$$

$$\frac{\partial \langle u_x \rangle}{\partial t} = -\frac{\partial \langle P \rangle}{\partial x} - \frac{\partial \langle u_x'^2 \rangle}{\partial x}$$
$$+ 3\pi \nu_g \lambda \left\langle \phi \left(v_x - u_x \right) \left(1 + 0.15 \mathrm{Re}^{0.687} \right) \right\rangle \qquad (23)$$

Equation (22) says that the mean gas velocity is a constant in space. If we specify the inlet mean gas velocity as a constant in time, then the mean gas velocity throughout the domain is constant in both space and time. This makes solving the gas momentum equation unnecessary unless one is interested in the pressure.

Closure

Several models are used to close the above set of equations. First, a maximum entropy approach[15, 16, 17] is taken to close the higher-order moments, such as the third-order velocity moment in the advection term in equation (20). The maximum entropy principle states that of all possible PDFs consistent with a set of given (moment) constraints, the one PDF that is most unbiased is the one with the most entropy. All known information is included in the form of the constraints, with no extraneous information that might tend to bias the PDF. We can then integrate the maximum entropy PDF to obtain values for the higher-order moments.

Additional modeling is required for the cross-phase/same-component moments that appear in the equations. In the derivation of the spray equation, the gas velocity was not included as part of the set of characteristics that describes a drop. This amounts to an independence assumption between the two phases which is non-physical. We must therefore develop a model for these moments. This will be done by choosing a functional form for the correlation coefficient. The correlation coefficient is defined as

$$Corr_x = \frac{\langle u_x v_x \rangle_n - \langle u_x \rangle \langle v_x \rangle_n}{\sigma_{u_x} \sigma_{v_x,n}} \qquad (24)$$

where σ_{u_x} and σ_{v_x} are the gas and drop velocity variances, respectively, in the nth diameter bin. In general, the correlation coefficient can have any value between negative one and positive one, inclusive. The physics of this problem, however, dictate that the coefficient must be bounded between zero and positive one. Physically, this is because a positive increase in the drop velocity will produce a positive increase in the gas velocity.

Perfect correlation between the velocities of the two phases implies that their means and variances are identical. Any differences would reduce the degree of correlation, and since those differences can be large, we assume that there is zero correlation if either the difference of the means or the differences of the variances are infinite. We also know that the correlation depends upon the drop size. The velocities of small drops ten to be more correlated with the gas velocity because of their small relaxation times,

whereas the velocities of larger drops, which take longer to respond to fluctuations in the gas phase, tend to be less correlated. All of these considerations are accounted for if the correlation coefficient is modeled as an exponential function

$$Corr_x = \exp\left(-C_o \frac{\tau_n}{\tau_g}\right) \qquad (25)$$

where the ratio of time scales represents a droplet Stokes' number. C_o is an adjustable constant that must be determined from experiment, τ_n is the drop relaxation time, and τ_g is the gas-phase time scale. Short drop relaxation times will have velocities that are highly correlated with the gas velocity. Thus, drops in the limit of having no mass will be perfectly correlated. Large drops with long relaxation times will not be as well correlated. The gas time scale is taken to be the shorter of the mean residence time of a drop in a turbulent eddy with size equal to the turbulent length scale, or the turbulent time scale. If the residence time within an eddy is short, that means that there is strong slip between the drops and the gas, resulting in a low velocity correlation. On the other hand, if the mean residence time is long, then the correlation is based upon the eddy lifetime, as defined by the turbulent time scale.

To find the turbulent time and length scales, and to close the Reynolds stress term in equation (23), we introduce a $k-\varepsilon$ model that has been modified to account for the presence of the drops. Applying constraints (17), the governing equations for the model are

$$\frac{\partial k}{\partial t} + \frac{\partial(k\langle \bar{u}\rangle)}{\partial x} = -\varepsilon + \dot{W}_s + \frac{\partial}{\partial x}\left[\left(v_g + \frac{v_t}{\xi_k}\right)\frac{\partial k}{\partial x}\right] \qquad (26)$$

$$\frac{\partial \varepsilon}{\partial t} + \frac{\partial(\varepsilon\langle \bar{u}\rangle)}{\partial x}$$
$$= \frac{-C_{\varepsilon2}\varepsilon + C_{\varepsilon3}\dot{W}_s}{T} + \frac{\partial}{\partial x}\left[\left(v_g + \frac{v_t}{\xi_\varepsilon}\right)\frac{\partial \varepsilon}{\partial x}\right] \qquad (27)$$

where T is the turbulence time scale,

$$v_t = \frac{C_\mu k^2}{\varepsilon} \qquad (28)$$

and

$$C_\mu = 0.09 \quad C_{\varepsilon2} = 1.92$$
$$C_{\varepsilon3} = 1.5 \quad \xi_k = 1.0 \quad \xi_\varepsilon = 1.3 \qquad (29)$$

where the constant values are the same as in Amsden *et. al.*[3] Notice that the terms containing the production of turbulent kinetic energy are identically zero under the imposed geometric constraints. The term

$$-\dot{W}_s = \langle F'_x u'_x\rangle + \langle F'_y u'_y\rangle \qquad (30)$$

is the negative of the rate at which the turbulent eddies are doing work dispersing the drops. If $\dot{W}_s < 0$, then the turbulent kinetic energy is being transferred from the gas to the drops, and if $\dot{W}_s > 0$, the drops are losing their energy and transferring it to the gas in the form of turbulent kinetic energy. F'_x and F'_y are the fluctuations from the mean force in the x- and y-directions acting on the gas by the drops. Equation (30) is computed by

$$\dot{W}_S = -\int_{\alpha'} F(\bar{\alpha};t)\,\bar{F}\cdot\bar{u}'d\bar{\alpha}' \qquad (31)$$

For compactness, we do not show the final expression here as it is rather lengthy. However, we should note that it contains numerous nonlinear terms that would be too expensive to compute directly. To remedy this, each term was expanded in a Taylor series thus reducing the time required to compute these terms.

Solution

The moment equations are solved using an implicit, first-order, upwind scheme for the spatial derivatives and a second-order backwards difference for the time derivatives. A first-order scheme was chosen for the spatial derivatives due to the difficulties associated with solving moment equations. Moment variables have relations among them that must be preserved, constraining their values. For example, the relation between the first and second moments of a PDF is

$$\langle X^2\rangle - \langle X\rangle^2 \geq 0 \qquad (32)$$

where X is any random variable. If this relation is not maintained, then the numerical solution may either become unstable or give non-physical answers. Second-order numerical solutions of hyperbolic equations can cause oscillations in the solution in regions of strong gradients, even when artificial dissipation is added. Being non-physical, those oscillations could cause the numerical solution of the variance to become negative, corrupting the remainder

of the solution. Therefore, the first-order numerical scheme is presently used.

Results

To provide a comparison between the MEMC model and more conventional methods, a Lagrangian simulation of the quasi-one-dimensional spray is performed. Parcels, each representing 100 drops, are tracked from the injector along their trajectories. Because the mean gas velocity is a constant in space and time, the gas momentum and continuity equations are not solved, though the $k-\varepsilon$ model is used to simulate the turbulence, giving each drop a random "kick" over a duration equal to the eddy turnover time or the drop residence time, whichever is shorter. This is similar to what is done in other Lagrangian simulations (e.g., KIVA[3]). The trajectory equations are solved by a fourth-order Runge-Kutta method. Results for four simulations are averaged and only shown for 0.03 sec of flow time. This is due to the extensive time required to compute Lagrangian statistics at longer flow times.

Table 1 lists the moments used to specify the droplet PDF at the injector and the gas phase

Figure 2 Injector diameter PDF

Figure 3 Expected drop number density

Quantity	Value	Quantity	Value
λ	$1000 \ \frac{drops}{cm^3}$	σ_{v_x}	$3.0 \ m/s$
$\langle \phi \rangle$	$100 \ \mu m$	σ_{v_y}	$3.0 \ m/s$
$\langle \phi^2 \rangle$	$150 \ \mu m^2$	$\langle u_x \rangle$	$6.0 \ m/s$
$\langle \phi^3 \rangle$	$300 \ \mu m^3$	$\langle u_y \rangle$	$0.0 \ m/s$
$\langle v_x \rangle$	$30 \ m/s$	σ_{u_x}	$0.3 \ m/s$
$\langle v_y \rangle$	$0.0 \ m/s$	σ_{u_y}	$0.3 \ m/s$

Table 1 Injector Conditions

characteristics. At the injector, there is a 24 m/s slip velocity between the phases, well into the non-linear drag regime. The diameter PDF is shown in Figure 2. This PDF was produced using the Maximum Entropy Formalism with the constraints listed in Table 1. The velocity PDFs are Gaussian, which is also the maximum entropy solution for the given moment constraints in Table 1. The inlet condition for the turbulent kinetic energy corresponds to a RMS value of five percent of the mean gas velocity and the rate of dissipation of turbulent kinetic energy is $\varepsilon = k / 100 \ sec$.

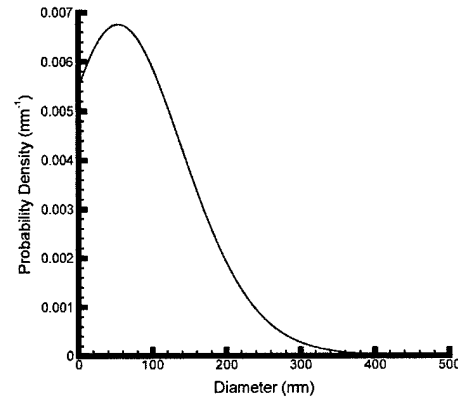Figure 3 shows profiles of the mean number density at various instants in time. The spray
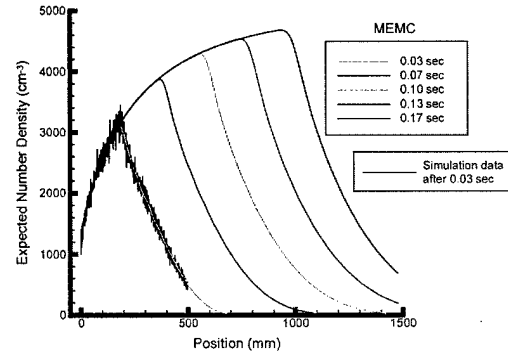
propagates through the domain as a concentration wave as indicated by the advancement of the leading edge. Starting with 1000 drops/cm³ at the injector, the expected number density increases downstream as the drops decelerate in the slower moving gas until we reach the leading edge where it drops off sharply. There is excellent agreement with the results from the Lagrangian simulation at 0.03 sec. Notice, however, the amount of noise present in the simulation data. This is indicative of this type of calculation where it is necessary to compute discrete data, whereas in the MEMC model, we get a smooth curve representing the averaged data.

At the leading edge, the mean number density is quite low. When drops first arrive at some spatial location, only a few are present, those that were large enough not to have been greatly influenced by drag. This is shown in Figure 4 where the expected drop diameter is plotted At the leading edge, there is a greater mean drop diameter. This is caused by the strong slip velocity present in the flow, decelerating all but the most massive drops. As we move upstream, we
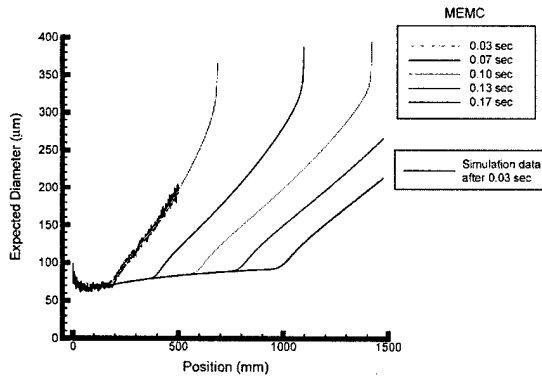
Figure 4 Expected drop diameter

Figure 6 Expected drop axial velocity

encounter the smaller drops that were quickly decelerated.

Figure 5 shows how the standard deviation of the diameter PDF evolves. At the leading edge, the standard deviation is large due to the fact that there are so few drops out on the wave front. Those drops present are large due to the size-velocity correlation that
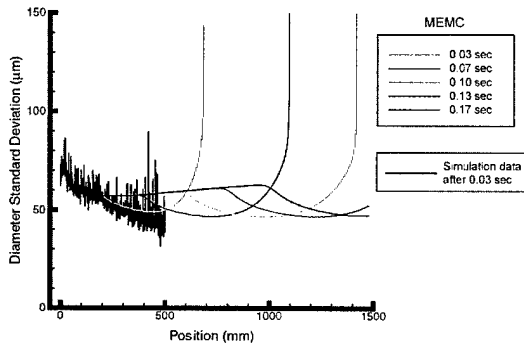

Figure 5 Drop diameter standard deviation

has developed. Figure 2 shows that there is a wide range of large diameters that those drops have. It can be argued that the dip in the standard deviation curve behind the leading edge is a phenomenon that arises from the spatial spreading of the drops that were initially injected, however, due to the diffusion in the numerical solution at the leading edge, this effect may appear more significant than it really is. Finally, notice that for this second-order moment, the amount of noise in the simulation data has increased over that shown in Figure 3. This is due to the fact that it is more difficult to obtain higher-order statistics from a simulation, often creating more ambiguity in the data. Despite the noise, however, we see that the MEMC model agrees well with the simulation.

Figure 6 shows the mean drop axial velocity profiles. The region closest to the injector is where the
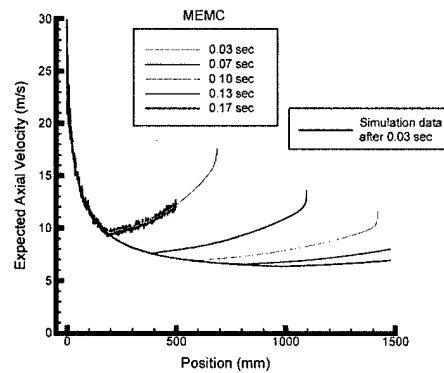
highest velocity slip occurs. There are a number of drops passing through this region that are moving faster than the mean gas velocity. Due to their lower masses, most of those drops rapidly decelerate, reducing the mean velocity towards the mean gas velocity. At the leading edge, however, the mean velocity increases. To have reached the leading edge, those drops had to be the fastest coming out of he injector, and because they are also some of the largest, they haven't been affected by drag as much as the smaller drops. As the wave front continues to move forward, those large drops slow as evidenced by the decrease in the mean velocity at the front as time goes on.

Figures 7 and 8 show the standard deviations of the axial and transverse velocity distribution functions. The largest standard deviations occur near the injector
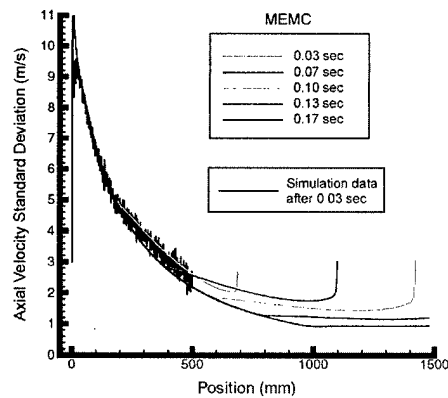

Figure 7 Drop axial velocity standard deviation

because the drops have not been influenced by the gas phase long enough to have approached the gas velocity. Downstream, the standard deviations rapidly decay until we reach the wave front. It will take a longer time for the larger drops to reach the gas velocity, but as the leading edge propagates, the standard deviations
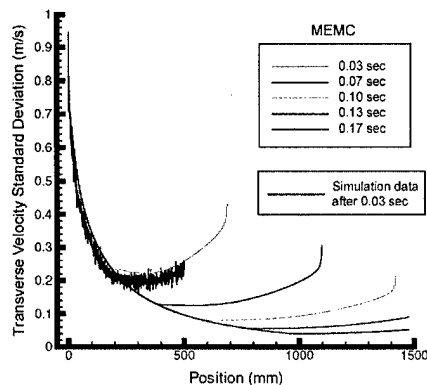
Figure 8 Drop transverse velocity standard deviation

become smaller and smaller. Comparisons with the Lagrangian simulation again show good agreement. This suggests that the submodels used to close the cross-phase/same-component velocity moments and term appearing in the turbulence equations representing the effects of the drops do a satisfactory job in allowing the overall model to predict the statistics of the spray.

Conclusions

We have incorporated the effects of nonlinear momentum exchange between the phases into a model which describes the evolution of a spray flow by solving a series of moment equations with a maximum entropy model. The model was tested for a quasi-one-dimensional spray flow. Results were obtained for several quantities of interest, including the expected drop number density, expected diameter, expected axial velocity, and various second-order moments. For comparison, a Lagrangian simulation was performed which showed good agreement with the MEMC results. While the point was not emphasized in the present work, we determined that the MEMC model requires less computational time to provide similar statistics as a simulation. Finally, we showed that the submodels used to describe the cross-phase velocity moments and the turbulence modification allow the overall MEMC model to provide reasonable agreement with the simulation data.

References

1. Dukowicz, J. K., "A Particle-Fluid Numerical Model for Liquid Sprays," *J. Comp. Phys.*, vol. 35, pp 229-253, 1980.
2. Gosman, A. D., & Ioannides, E., "Aspects of Computer Simulation of Liquid Fueled Combustors," *J. Energy*, vol. 7, pp. 482-490, 1983.
3. Amsden, A. A., O'Rourke, P. J., & Butler, T. D., "KIVA-II: A Computer Program for Chemically

Reactive Flows with Sprays," Los Alamos National Laboratory, Report No. LA-11560-MS, Los Alamos, NM, 1989.
4. Berlemont, A., Desjonqueres, P., & Gouesbet, G., "Particle Lagrangian Simulation in Turbulent Flows," *J. Multiphase Flow*, vol. 16, pp. 19-34, 1990.
5. Williams, F. A., "Spray Combustion and Atomization," *Phys. Fluids*, vol. 1, pp. 541-545, 1958.
6. Bracco, F. V., Gupta, H. C., Krishnamurthy, L., Santavicca, D. A., Steinberger, R. L., & Warshaw, V. "Two-Phase, Two-Dimensional, Unsteady Combustion in Internal Combustion Engines; Preliminary Theoretical-Experimental Results," SAE paper 760114, 1976.
7. Westbrook, C. K., "Three Dimensional Numerical Modeling of Liquid Fuel Sprays," *Sixteenth Internat. Symp. Combust.*, Cambridge, 1976.
8. Gupta, H. C., & Bracco, F. V., "Numerical Computations of Two-Dimensional Unsteady Sprays for Application to Engines," *AIAA J.*, vol. 16, pp. 1053-1061, 1978.
9. Haselman, L. C., & Westbrook, C. K., "A Theoretical Model for Two-Phase Fuel Injection in Stratified Charge Engines," SAE paper 780318, 1978.
10. Sirignano, W. A., "The Formulation of Spray Combustion Models: Resolution Compared to Droplet Spacing," *J. Heat Transfer*, vol. 108, pp. 633-639, 1986.
11. Archambault, M. R. & Edwards, C. F., "Computation of Spray Dynamics By Direct Solution of Moment Transport Equations," AIAA paper 2000-0197, 2000.
12. Edwards, C. F., & Marx, K. D., "Single-Point Statistics of Ideal Sprays, Part I: Fundamental Descriptions and Derived Quantities," *Atomization and Sprays*, vol. 6, pp. 499-536, 1996.
13. Williams, F. A., *Combustion Theory*, 2nd ed., The Benjamin/Cummings Publishing Company, Menlo Park, CA, 1985.
14. O'Rourke, P. J., "Collective Drop Effects on Vaporizing Liquid Sprays," Ph.D. thesis, Princeton University, Princeton, NJ, 1981.
15. Archambault, M. R., "A Maximum Entropy Moment Closure Approach to Modeling the Evolution of Spray Flows," Ph.D. thesis, Stanford University, Stanford, CA, 1999.
16. Jaynes, E. T., "Information Theory and Statistical Mechanics," *Phys. Review*, vol. 106, pp. 620-630, 1957.
17. Kapur, J. N., & Kesavan, H. K., *Entropy Optimization Principles with Applications*, Academic Press, Boston, MA, 1992.